IEEE Photonics Journal
An IEEE Photonics Society Publication

Open Access

Balanced Detection of 100-Gb/s Optical OFDM Signals With SSBI Cancellation Based on Fused-Type Fiber Mode-Selective Coupler

Volume 10, Number 5, September 2018

Ying Qiu
Ming Luo
Zhixue He
Xiang Li

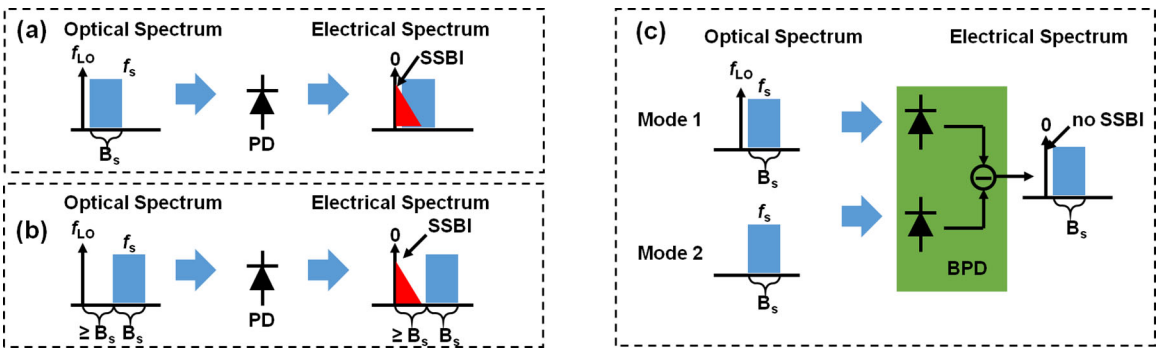

DOI: 10.1109/JPHOT.2018.2866574
1943-0655 © 2018 IEEE

Balanced Detection of 100-Gb/s Optical OFDM Signals With SSBI Cancellation Based on Fused-Type Fiber Mode-Selective Coupler

Ying Qiu,[1,2,3] **Ming Luo,**[1,2,3] **Zhixue He,**[2,3] **and Xiang Li** [2,3]

[1]Wuhan National Laboratory for Optoelectronics, Huazhong University of Science and Technology, Wuhan 430074, China
[2]State Key Laboratory of Optical Communication Technology and Networks, Wuhan Research Institute of Posts Telecommunications, Wuhan 430074, China
[3]National Optoelectronics Innovation Center, Wuhan Research Institute of Posts and Telecommunications, Wuhan 430074, China

DOI:10.1109/JPHOT.2018.2866574

Manuscript received July 6, 2018; revised August 10, 2018; accepted August 18, 2018. Date of publication August 22, 2018; date of current version October 4, 2018. This work was supported in part by the National Natural Science Foundation of China (61705171), in part by the Key Projects of Natural Science Foundation of Hubei Province (2016AAA012), in part by the 2017 Wuhan Basic Applied Research Projects 2017010201010101 and 2017010201010100, and in part by the Natural Science Foundation of Hubei Province under Grants 2015CFA063, 2016CFB302, and 2016CFB597. Corresponding author: Xiang Li (e-mail: lixiang@wri.com.cn).

Abstract: We propose a signal-to-signal beating interference (SSBI) cancellation scheme in two-mode fiber (TMF) transmission system based on balanced detection without requirement of a guard band. The SSBI can be eliminated based on the mode selectivity characteristic of mode coupler. The mode selectivity in mode coupler relies on the coupling behavior between the fundamental mode LP_{01} and the first-order mode LP_{11}, which is highly dependent on the spatial orientation of the fiber modes. We design and fabricate a fused-type fiber mode coupler (FFMC) based on circular-core TMF. Based on the fabricated FFMC, we experimentally demonstrate a multi-band 100-Gb/s optical orthogonal frequency division multiplexing signal transmission over 10-m TMF with SSBI cancellation. Significant performance improvement is observed when compared with conventional direct detection scheme under the condition of insufficient bandwidth of a guard band.

Index Terms: Fiber optics communications, optical couplers, two-mode fiber transmission.

1. Introduction

Driven by the emerging mobile and cloud applications, transmission of 100 Gb/s per single wavelength is necessary for future intra-datacenter interconnects (DCIs) covering transmission distances from tens of meters to several kilometers [1], [2]. Although coherent optical transmission modules at 100 Gb/s or 400 Gb/s can satisfy the growing capacity demands in DCIs, they are designed for long-haul transmission scenarios, which are suffered from high digital signal processing (DSP) complexity and cost [3]–[5]. Research efforts have been put on to improve the single wavelength data rate to 100 Gb/s based on intensity modulation and direct detection (IMDD) technique due to its simple structure and low cost [6]–[10]. However, only the amplitude of the optical field is used to modulate the signal, resulting in low spectral efficiency. The transmission distance is also

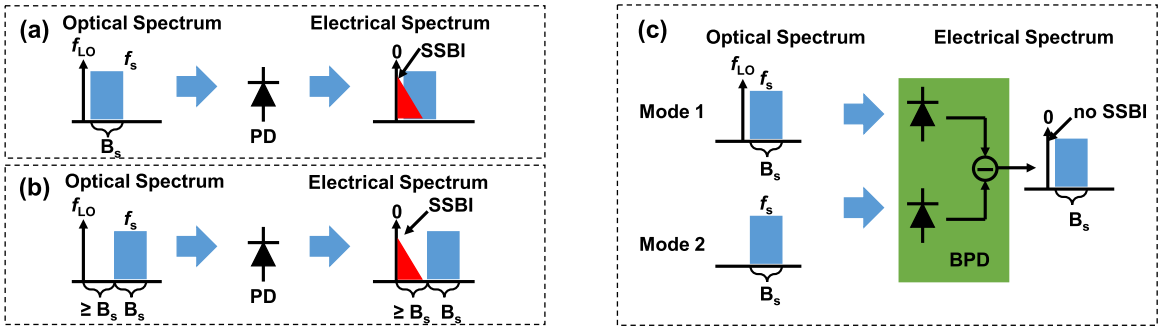

Fig. 1. The pilot-supported direct-detection scheme. (a) SMF without guard band. (b) SMF with guard band. (c) TMF without guard band.

limited in IMDD technique based system at 1550 nm due to the chromatic dispersion induced power fading. In order to achieve complex modulation with direct detection, pilot-supported direct detection schemes have been proposed with various modulation formats [11]–[15]. Moreover, chromatic dispersion compensation can be realized in pilot-supported direct detection schemes by electrical field extraction of the OFDM signals.

In conventional pilot-supported direct-detection single mode fiber (SMF) transmission systems, the performances are seriously affected by the signal-to-signal beat interference (SSBI) [14]. Although several advanced DSP algorithms such as Kramers–Kronig receiver and SSBI iterative cancellation have been proposed to deal with the SSBI issue, they all have the disadvantages of complex nonlinear digital operation with incomplete SSBI mitigation [16]–[18].

SSBI estimation and cancellation can also be achieved in optical domain [19]–[22]. However, optical filter with steep edge is required at the receiver side to remove the pilot carrier, which increases the system complexity and wastes the spectral efficiency due to the frequency guard band between the optical signal and pilot carrier [19], [20]. We have recently proposed and experimentally demonstrated balanced detection scheme after multi-core fiber (MCF) and two-mode fiber (TMF) transmission systems with SSBI elimination [21], [22]. Compared with MCF, TMF has the advantages of large effective areas and convenient connection to the SMF. As an extension of our previous work in [21], this paper includes the following two new contributions: (i) we provide more details on the design and theoretical analysis of the mode-selective fused-type fiber mode coupler (FFMC). The mode converting and coupling situation affected by the polarization angle of the incident light is analyzed. The optimal value of coupling length, TMF core diameter and TMF cladding diameter of the FFMC is obtained by simulation; and (ii) the experiment results are extensively extended by including the performance of OFDM signal in each subband and effects of guard band in the pilot-supported balanced-detection TMF transmission system.

The remainder of this paper is organized as follows: Section 2 presents the principle of SSBI cancellation in the TMF transmission system. Section 3 describes the design and characterization of the FFMC. Sections 4 and 5 discuss the experiment setup and results of the TMF transmission for 100-Gb/s multi-band orthogonal frequency division multiplexing (OFDM) signals. Finally, conclusions are drawn in Section 6.

2. Principle of SSBI Cancellation

Conventional direct-detection scheme based on optical carrier and signal beating in SMF transmission is shown in Fig. 1(a). If the frequency difference between the optical carrier and signal is smaller than the bandwidth of signal Bs, the received electrical signal will be contaminated by the SSBI, which will degrade the system performance significantly, as shown in Fig. 1(a). Although several SSBI mitigation methods have been proposed, they cannot completely remove the SSBI at the cost of additional DSP complexity. Therefore, the more efficient method is to use guard band

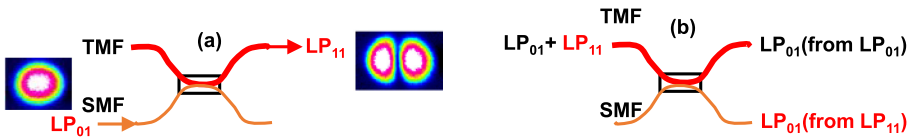

Fig. 2. The function of fused fiber mode coupler. (a) LP_{01} mode from SMF arm convert to LP_{11} mode in TMF arm. (b) The LP_{01} and LP_{11} modes in TMF are de-multiplexed into LP_{01} modes in two arms.

in direct-detection scheme. As described in Fig. 1(b), SSBI can be completely removed as long as the bandwidth of the guard band is larger than the bandwidth of signal Bs at the cost of waste of spectral efficiency.

The proposed scheme to completely remove the SSBI in TMF without sacrifice of spectral efficiency is shown in Fig. 1(c). We first transmit the optical carrier and signal as two independent modes (LP_{01} and LP_{11}) in the TMF. If the mode selectivity characteristics exist, one output may include the combination of optical carrier and signal. In this case, the optical fields can be expressed as $C + S$, where C and S represent the optical carrier and signal, respectively. Similarly, another output may include only the optical signal S. Therefore, when the two output streams are launched into the two input ports of balanced photo detector (BPD), the output of the BPD can be described as $(C + S)^2 - S^2 = C^2 + 2CS$. The first term in the right side is the direct current (DC) part of the received signal which can be eliminated easily by DC block. The second term in the right side is the desired electrical field of the signal, which is amplified by the optical carrier. In this way, the SSBI can be removed without requirement of guard band. From above analysis, we can see that in order to remove the SSBI after TMF transmission, specially designed mode coupler is required to achieve the mode selectivity as described in Fig. 1(c).

3. Device Design and Characterization

The principle of mode converting and mode coupling of FFMC is shown in Fig. 2. As shown in Fig. 2(a), the FFMC is composed of SMF and TMF which are fused by traveling flame along the longitudinal direction, enabling the light coupled from one piece of fiber to another piece. The LP_{01} mode from SMF arm is converted to the LP_{11} mode in TMF arm. After traveling a length of TMF with another FFMC for mode de-multiplexer, the LP_{01} mode in TMF arm is still LP_{01} mode, existing with the residual LP_{11} mode, as shown in Fig. 2(b). The SMF arm, however, only includes the LP_{01} mode which is transformed from LP_{11} mode in TMF arm. The LP_{01} and LP_{11} mode patterns are both observed through Charge-coupled Device (CCD) showing in Fig. 2(a). We design and fabricate a FFMC based on a single mode fiber and a circular core two-mode fiber replacing the elliptical core two-mode fiber [23], [24] to better controlling the coupling situation of the two modes. It is noted that the residual LP_{11} in the de-multiplexer output due to the mode selectivity can be used to eliminate SSBI, as described in Fig. 1. The circular TMF is fabricated by Fiberhome Corporation, which supports LP_{01} mode and two degenerate LP_{11} modes, referring as LP_{11a} and LP_{11b} modes. The TMF is based on step index structure with trench, and is optimized to effectively stabilize LP_{11} mode and cutoff other higher modes.

We analyze the coupling behavior of LP_{01} and LP_{11} modes in FFMC by FDTD (finite difference time domain) in simulation. Fig. 3(a) is the 2D model of FFMC. The cladding diameter and index of SMF and TMF are 125 μm and 1.444. The core diameter of the two fibers are 9 μm and 13.5 μm, respectively. The refractive index differences of the two fibers are 0.3% and 0.46%, respectively. The effective refractive index of LP_{01} and LP_{11} mode as a function of the taper diameter is shown in Fig. 3(b). The slope difference of effective refractive index between LP_{01} and LP_{11} mode is relatively small. Therefore, the phase matching condition is hard to be destroyed due to fabrication error [25]. In order to avoid the converted LP_{11} mode light in TMF converting back to SMF, the diameter, cladding diameter and coupling length should be properly designed.

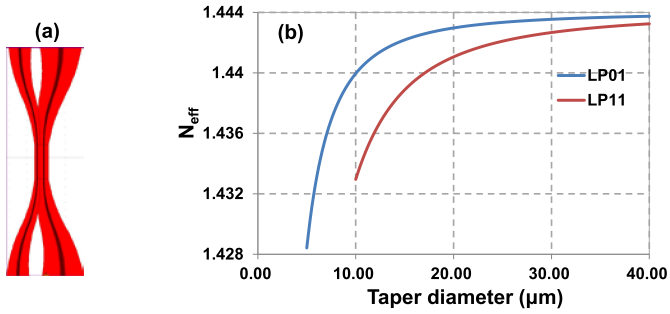

Fig. 3. (a) 2D model of FFMC. (b) Effective refraction index of LP_{01} and LP_{11} modes as a function of taper diameter in fused area.1. The circular TMF is fabricated by Fiberhome Corporation, which supports LP_{01} mode and two degenerate LP_{11} modes, referring as LP_{11a} and LP_{11b} modes. The TMF is based on step index structure with trench, and is optimized to effectively stabilize LP_{11} mode and cutoff other higher modes.

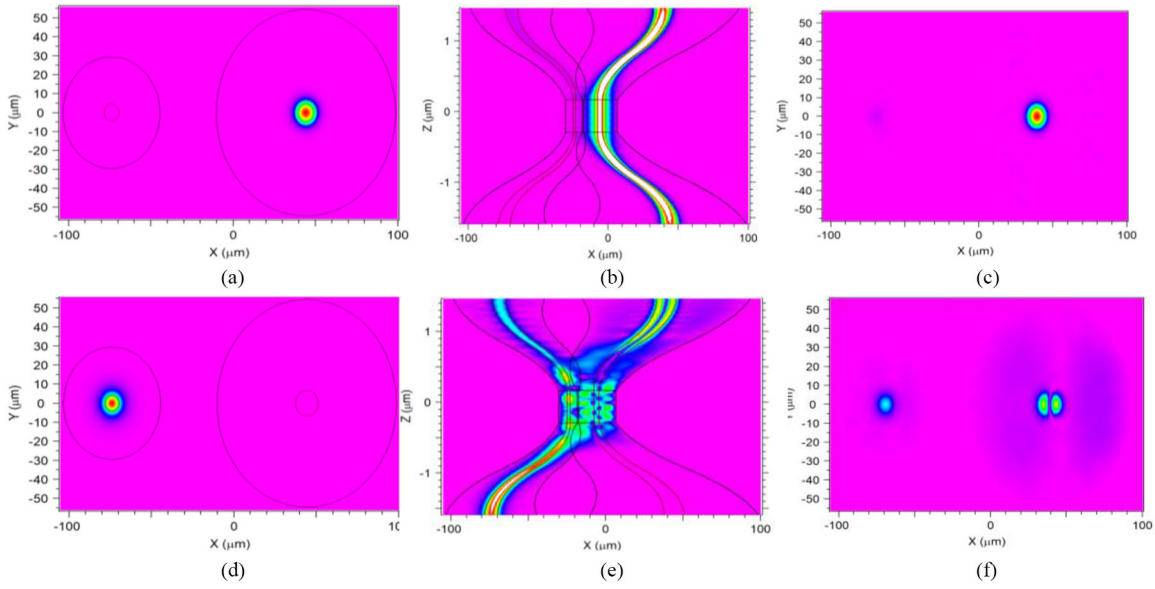

Fig. 4. Transmission path and mode field of FFMC. (a) LP_{01} input mode field in TMF arm. (b) Transmission path in TMF arm. (c) Output mode field when the input LP_{01} mode in TMF arm. (d) LP_{01} input mode field in SMF arm. (e) Transmission path in SMF arm. (f) Output mode field when the input LP_{01} mode in SMF arm.

Firstly, we study how the modes are transmitting and coupling when LP_{01} mode is input into the FFMC. The LP_{01} mode at the TMF input surface is shown in Fig. 4(a). The mode transmits through the TMF and maintain LP_{01} mode in fused area, as shown in Fig. 4(b). Therefore, the output mode field is still LP_{01} mode as shown in Fig. 4(c). However, when the LP_{01} mode is launched into the SMF port (see Fig. 4(d)), the mode coupling occurs, and part of energy transform into the LP_{11} mode as shown in Fig. 4(e). The output mode fields containing both LP_{01} and LP_{11} modes are shown in Fig. 4(f).

We then analyze the effects of polarization angle of input light on the coupling behavior when connecting two FFMCs, as shown in Fig. 5. We investigate the output power of FFMC when the light of LP_{01} mode is launched into the input port I and II, respectively. The normalized power at the output port III and IV by simulation is shown in Fig. 6. It can be seen that when the light is launched into the port I, the output power is close to 1 and 0 at port III and port IV at all different polarization angles. However, when the light is launched into the port II, the output power at port III and IV is complementary with the change of polarization angle. We also conduct an experimental

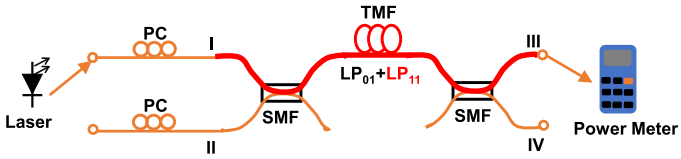

Fig. 5. Simulated and experimental schemes to measure the conversion efficiency of LP_{01} and LP_{11} in TMF.

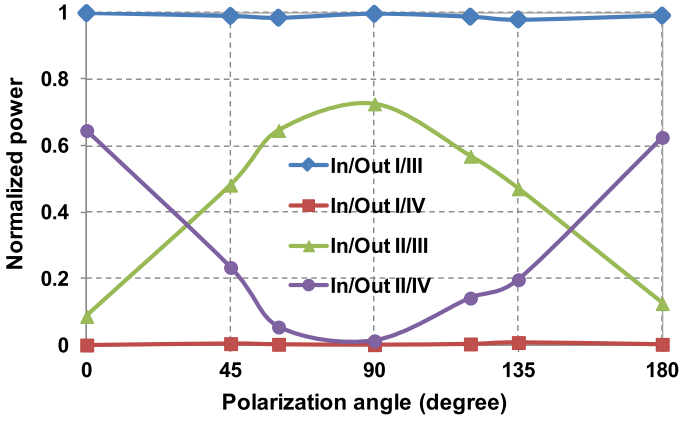

Fig. 6. Normalized Power versus polarization angle of input light.

TABLE 1
Optical Power at Output Port of FFMC With Different Input Port

Input/Output Port	III	IV
I	12.85 dBm	-8.02 dBm
II	5.01 dBm(Pmax)~3.16 dBm(Pmin)	-2.5 dBm (Pmin)~3.33 dBm (Pmax)

measurement on the effects of polarization angle of input light based on the scheme in Fig. 5. The output power of laser is 13.27 dBm and the polarization orientation of the light is adjusted by a polarization controller (PC). The output power at port III and IV is measured by an optical power monitor. The experimental results are similar to the simulation results, as shown in Table 1. In order to achieve the SSBI cancellation, two requirements are necessary: (1) high extinction ratio at the output ports when the light is launched into the port I; and (2) equal optical power at the output ports when the light is launched into the port II. It can be seen in Table 1 that these two requirements can be satisfied by adjusting the polarization angle of the input light.

Finally, we study the effects of cladding diameter and core diameter of fused-area TMF on the mode conversion efficiency when that light is input from the port II. It is noted that when the light is launched into the port I, no mode conversion occurs. By calculating the output power ratio between the LP_{11} and LP_{01} modes, the optimal values of coupling TMF cladding diameter and coupling TMF core diameter are 25.0 μm and 3.1 μm with power ratio of 10 dB as shown in Fig. 7(a) and (b), respectively.

4. Experimental Setup

The experimental setup to verify the effectiveness of our proposed balanced-detection scheme with fabricated FFMC after TMF transmission is shown in Fig. 8. One external-cavity laser (ECL) with line-width less than 100 kHz is fed into an optical in-phase/quadrature-phase (IQ) modulator, which is modulated by the OFDM signal. The OFDM signal with 16-QAM format is produced by an

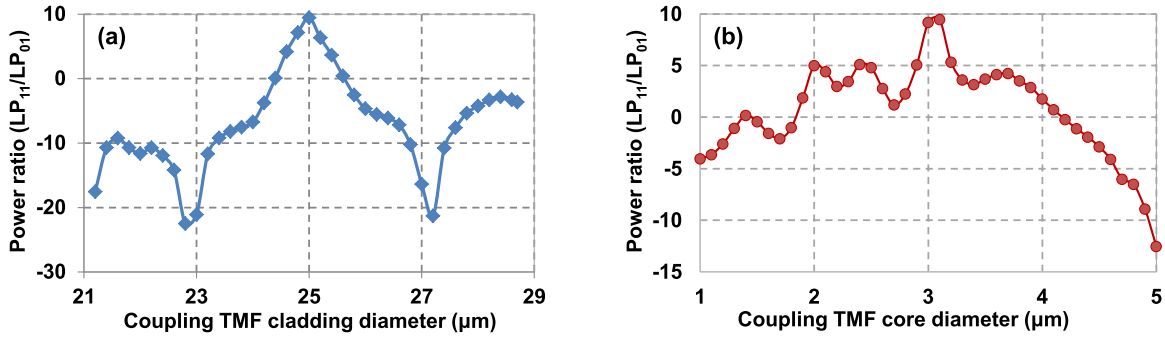

Fig. 7. (a) Fused area TMF cladding diameter optimization, optimum value = 25 μm. (b) Fused area TMF core diameter optimization, optimum value = 3.1 μm.

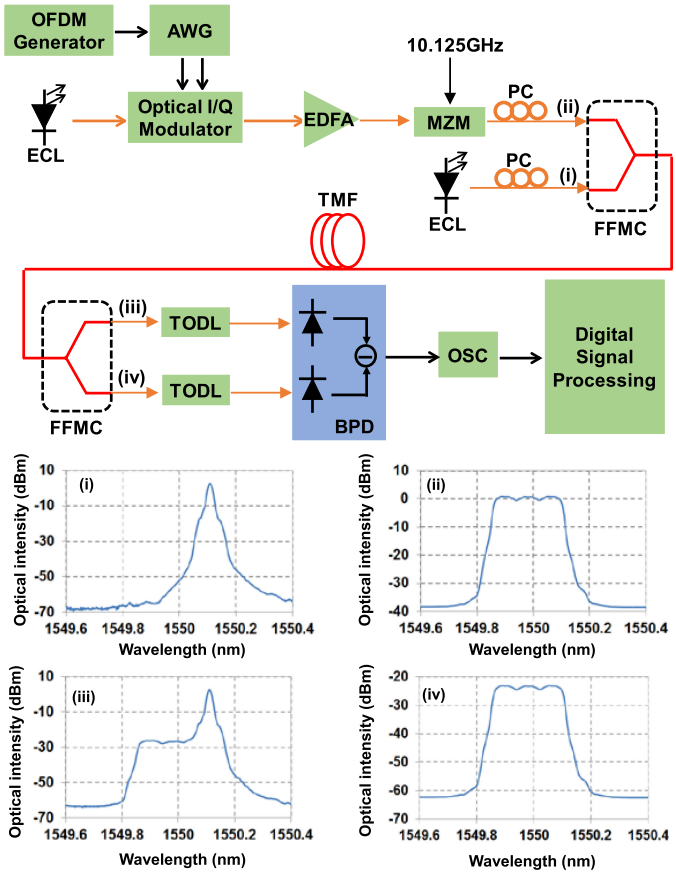

Fig. 8. Experimental setup of 100-Gb/s balanced-detection scheme without guard band in TMF transmission based on FFMC. The corresponding optical spectrum are shown in the inset (i) to (iv).

arbitrary waveform generator (AWG, Tektronix 7122C) operating at 12 GSa/s. For the generation of electrical OFDM signal, the inverse fast Fourier transform (IFFT) size is 256 where 210 subcarriers are filled with data. The middle 2 subcarriers are unloaded to avoid the DC influence. 2 subcarriers are selected as the pilots to correct the laser phase noise. The 1/32 of the OFDM symbol period is used as cyclic prefix (CP) to avoid the inter-symbol interference. After optical amplification by an Erbium doped fiber amplifier (EDFA), an intensity modulator (IM) is used to replicate the OFDM signal to three copies with driving sine wave signal at 10.125 GHz to enhance the net data rate.

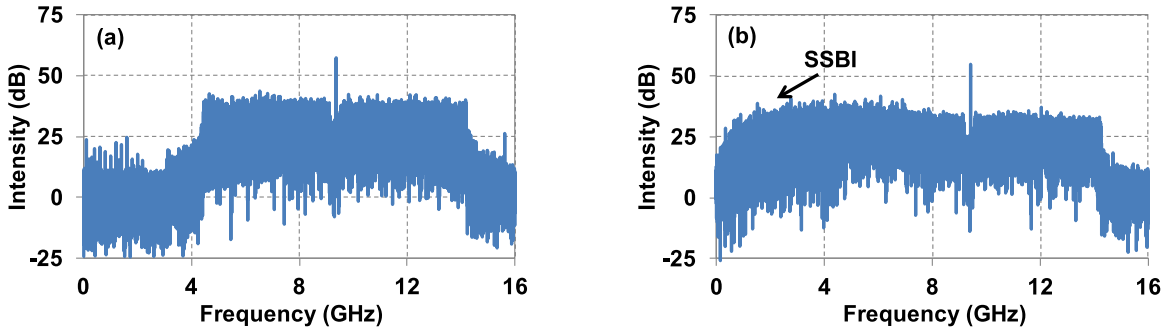

Fig. 9. The electrical spectrum of received OFDM signal at frequency difference of 9.5 GHz for (a) w/SSBI cancellation and (b) w/o SSBI cancellation.

The generated three-subband optical OFDM signals are then launched into one port of the FFMC. Another ECL with 16 GHz frequency shift is acted as an optical carrier and launched into another port of the FFMC directly. Two polarization controllers (PCs) are used to adjust the polarization states of optical carrier and signals at the transmitter side. After transmission over 10-m TMF, the optical carrier and signals are de-multiplexed by another FFMC. It is noted that the transmission distance is limited to be 10 meters in this experimental demonstration due to only 10-m TMF is available with small coupling ratio. Longer transmission distance can be achieved by specially designed weakly-coupled few-mode fiber [26]. The inset of Fig. 8 shows the optical spectrum at the corresponding point in the experimental setup. It is noted that the optical tunable delay lines are used to synchronize the optical carrier and optical OFDM signals. The two streams are launched into the two ports of the BPD to achieve optical-to-electrical conversion. Finally, the electrical signals are sampled by a digital storage oscilloscope (DSO Tektronix DSA72004B) operating at 50 GSa/s and processed off-line. The net data rate of the 3-subband OFDM signals considering the 7% FEC overhead is calculated as:

$$Net\,rate = 12\,\mathrm{GSa/s} \times \frac{206(\mathrm{Payload})}{256(\mathrm{FFT\,size}) + 8(\mathrm{CP})} \times 4\,\mathrm{bit/Sa} \times 3(\mathrm{No.\,of\,Subband})/1.07 = 105\,\mathrm{Gb/s}$$

5. Results and Discussion

The electronic spectrum considering only one OFDM subband with and without SSBI cancellation are shown in Fig. 9 when the frequency difference between the two ECLs is set at 9.5 GHz for one sub-band case. It is shown that the SSBI is completely cancelled in the low frequency region in Fig. 9(a) after optimizing the polarization states at the transmitter side. For comparison, the electrical spectrum without SSBI cancellation is shown in Fig. 9(b), where strong interference is observed in the low frequency region. We also investigate the effects of guard band for the one OFDM subband with and without SSBI cancellation. The Q^2 factor for two cases at different bandwidths of guard band is shown in Fig. 10. It is shown that the Q^2 factor stays at level of $\sim$19 dB for all the bandwidths of guard band with SSBI cancellation, which suggests that no SSBI is introduced after balanced detection. However, when the SSBI is not removed, the Q^2 factor drops significantly when the bandwidth of guard band is small. The penalty is reduced with the increasing of bandwidth of guard band. As long as the bandwidth of guard band is larger than the bandwidth of OFDM signal, the Q^2 factor can also reach $\sim$19 dB even without SSBI cancellation. The constellation points of the recovered OFDM signals at the corresponding points are also shown in the inset of Fig. 10.

Then we investigate the bit error rate (BER) versus carrier-to-signal power ratio (CSPR) for the three-subband OFDM signals. From Fig. 11, the optimal CSPR value is 12.7 dB, which is also used for the rest of experimental measurement. It is noted that the performance degradation at small value of CSPR is mainly due to the small beating electrical signal. However, when the CSPR

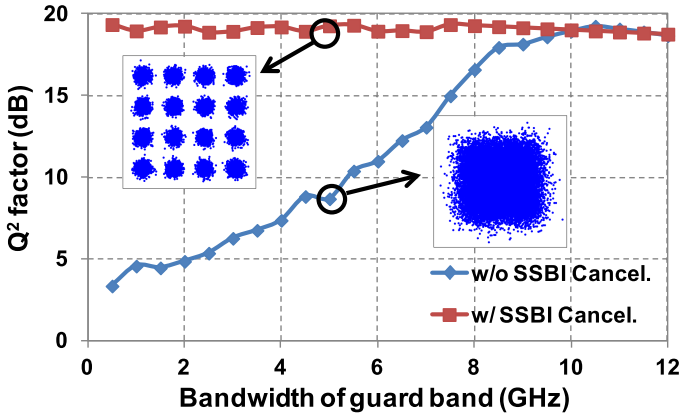

Fig. 10. Q^2 factor versus bandwidth of guard band with and without SSBI cancellation.

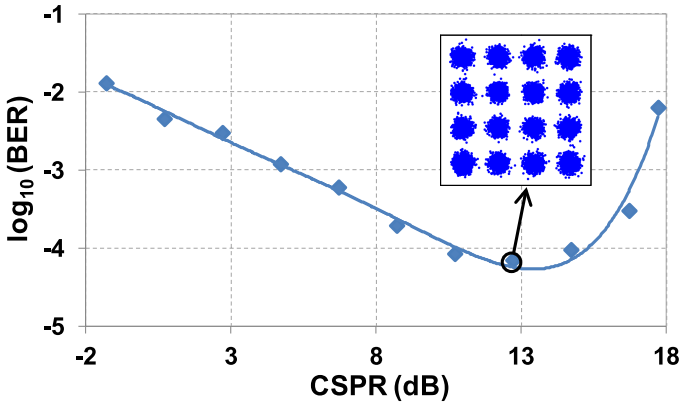

Fig. 11. BER performance versus CSPR for three-subband OFDMs signal after SSBI cancellation.

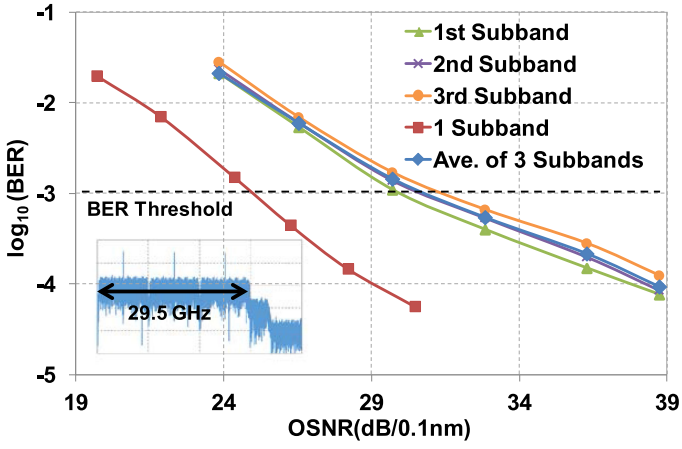

Fig. 12. BER performances of one-subband and three-subband OFDM signals after SSBI cancellation.

exceeds the optimal value, the performance is mainly affected by the nonlinear distortions in BPD due to large value of recovered electrical signals. Moreover, DC component induced thermal noise and signal to noise ratio of pilot carrier also becomes the dominant factors to affect the system performance. The BER performance of one-subband and three-subband OFDM signals versus optical signal to noise ratio (OSNR) is shown in Fig. 12. It is shown that small difference among the

BER performances of the OFDM signals in each subband can be observed, which is mainly due to the limited bandwidth of BPD at the receiver side. The average BER of three-subband OFDM signal can reach the BER threshold of 1×10^{-3} at OSNR value of $\sim$32 dB. Therefore, 100-Gb/s balanced-detection based our proposed scheme is achieved without requirement of guard band for SSBI cancellation. The electrical spectrum of the three-subband OFDM signal without guard band is also shown in the inset of Fig. 12.

6. Conclusions

In this paper, we have successfully demonstrated 100-Gb/s balanced-detection optical OFDM transmission over TMF based on specially designed FFMC with mode selectivity characteristic. The mode selectivity is realized by the coupling behavior between the fundamental mode LP_{01} and the first-order mode LP_{11} of the designed circular-core TMF based FFMC. Experimental results show that the SSBI can be successfully removed in our proposed balanced-detection scheme after TMF transmission without requirement of guard band. Our proposed scheme with specially designed FFMC has the potential in future high capacity short-reach intra-datacenter connections.

References

[1] C. Xie, "Scalability of optical technologies for growing exascale datacenters," in *Proc. Workshop Eur. Conf. Opt. Commun.*, 2017, WS1: Session3.

[2] K. Schmidtke, "Increasing datacenter bandwidth: A network or a technology issue?" in *Proc. Workshop Eur. Conf. Opt. Commun.*, 2017, WS1: Session3.

[3] J. Yu and X. Zhou, "Ultra-high-capacity DWDM transmission system for 100G and beyond," *IEEE Commun. Mag.*, vol. 48, no. 3, pp. S56–S64, Mar. 2010.

[4] K. Roberts, D. Beckett, D. Boertjes, J. Berthold, and C. Laperle, "100G and beyond with digital coherent signal processing," *IEEE Commun. Mag.*, vol. 48, no. 7, pp. 62–69, Jul. 2010.

[5] S. J. Savory, "Digital filters for coherent optical receivers," *Opt. Exp.*, vol. 16, no. 2, pp. 804–817, 2008.

[6] J. Lee *et al.*, "Demonstration of 112-Gbit/s optical transmission using 56GBaud PAM-4 driver and clock-and-data recovery ICs," in *Proc. Eur. Conf. Opt. Commun.*, 2015, Mo.4.5.4.

[7] C. Kottke, C. Caspar, V. Jungnickel, R. Freund, M. Agustin, and N. N. Ledentsov, "High speed 160 Gb/s DMT VCSEL transmission using pre-equalization," in *Proc. Opt. Fiber Commun. Conf. Exhib.*, 2017, W4I.7.

[8] J. Verbist *et al.*, "DAC-less and DSP-free PAM-4 transmitter at 112 Gb/s with two parallel GeSi electro-absorption modulators," in *Proc. Eur. Conf. Opt. Commun.*, 2017, W2A.16.

[9] Y. Xu, J. Yu, X. Li, and J. Xiao, "Demonstration of 4 lanes of 4 $\times$ 100 Gbps DMT transmission with channel spacing of 50-GHz compatible with DWDM," *Opt. Fiber Technol.*, vol. 36, pp. 227–230, 2017.

[10] J. Zhou *et al.*, "Interleaved single-carrier frequency-division multiplexing for optical interconnects," *Opt. Exp.*, vol. 25, no. 3, pp. 10586–10596, 2017.

[11] B. J. C. Schmidt, A. J. Lowery, and J. Armstrong, "Experimental demonstrations of electronic dispersion compensation for long-haul transmission using direct-detection optical OFDM," *J. Lightw. Technol.*, vol. 26, no. 1, pp. 196–203, Jan. 2008.

[12] A. J. Lowery and J. Armstrong, "Orthogonal-frequency-division multiplexing for dispersion compensation of long-haul optical systems," *Opt. Exp.*, vol. 14, no. 6, pp. 2079–2084, 2006.

[13] A. Li, D. Che, V. Chen, and W. Shieh, "Spectrally efficient optical transmission based on Stokes vector direct detection," *Opt. Exp.*, vol. 22, no. 13, pp. 15662–15667, 2016.

[14] W.-R. Peng *et al.*, "Theoretical and experimental investigations of direct-detected RF-tone-assisted optical OFDM systems," *J. Lightw. Technol.*, vol. 27, no. 10, pp. 1332–1339, May 2009.

[15] Y. Zhu, K. Zou, X. Ruan, and F. Zhang, "Single carrier 400G transmission with single-ended heterodyne detection," *IEEE Photon. Technol. Lett.*, vol. 29, no. 21, pp. 1788–1791, Nov. 2017.

[16] Z. Li *et al.*, "SSBI mitigation and the Kramers–Kronig scheme in single-sideband direct-detection transmission with receiver-based electronic dispersion compensation," *J. Lightw. Technol.*, vol. 35, no. 10, pp. 1887–1893, May 2017.

[17] C. Antonelli, A. Mecozzi, M. Shtaif, X. Chen, S. Chandrasekhar, and P. J. Winzer, "Polarization multiplexing with the Kramers–Kronig receiver," *J. Lightw. Technol.*, vol. 35, no. 24, pp. 5418–5424, Dec. 2017.

[18] T. Bo and H. Kim, "Kramers–Kronig receiver operable without digital upsampling," *Opt. Exp.*, vol. 26, no. 11, pp. 13810–13818, 2018.

[19] W. R. Peng, I. Morita, and H. Tanaka, "Enabling high capacity direct-detection optical OFDM transmissions using beat interference cancellation receiver," in *Proc. 36th Eur. Conf. Exhib. Opt. Commun.*, 2010, Tu.4.A.2.

[20] S. A. Nezamalhosseini, L. R. Chen, Q. Zhuge, M. Malekiha, F. Marvasti, and D. V. Plant, "Theoretical and experimental investigation of direct detection optical OFDM transmission using beat interference cancellation receiver," *Opt. Exp.*, vol. 21, no. 13, pp. 15237–15246, 2013.

[21] Y. Qiu, M. Luo, X. Li, Z. He, and Q. Yang, "SSBI-free 100 Gb/s direct detection based on fused-type mode-selective fiber coupler," in *Proc. Eur. Conf. Opt. Commun.*, 2017, Poster SessionI: SC4.59.

[22] Y. Wang *et al.*, "Beyond 100-Gb/s single-sideband direct detection using multi-core fiber and SSBI elimination," in *Proc. 22nd Opto-Electron. Commun. Conf., Photon. Global Conf.*, 2017, Oral 2-4K-2.
[23] K. Y. Song, I. K. Hwang, S. H. Yun, and B. Y. Kim, "High performance fused-type mode-selective coupler using elliptical core two-mode fiber at 1550 nm," *IEEE Photon. Technol. Lett.*, vol. 14, no. 4, pp. 501–503, Apr. 2002.
[24] N. Riesen and J. D. Love, "Weakly-guiding mode-selective fiber couplers," *IEEE J. Quantum Electron.*, vol. 48, no. 7, pp. 941–945, Jul. 2012.
[25] Y. Ding, L. Liu, C. Peucheret, and H. Ou, "Fabrication tolerant polarization splitter and rotator based on a tapered directional coupler," *Opt. Exp.*, vol. 20, no. 18, pp. 20021–20027, 2012.
[26] P. Sillard, M. Bigot-Astruc, D. Boivin, H. Maerten, and L. Provost, "Few-mode fiber for uncoupled mode-division multiplexing transmissions," in *Proc. 37th Eur. Conf. Exhib. Opt. Commun.*, 2017, Tu.5.Lecervin.7.